Electronic Supplementary Material (ESI) for Materials Horizons.

Supplementary Information

Organic indoor PV: Vanishing surface recombination allows for robust device architecture

Xueshi Jiang[1,2]*, Bernhard Siegmund[1,2]*, Koen Vandewal[1,2,3]*

1 Hasselt University, Institute for Materials Research (imo-imomec), Martelarenlaan 42, B-3500 Hasselt, Belgium

2 imec, imo-imomec, Wetenschapspark 1, B-3590 Diepenbeek, Belgium

3 Energyville, imo-imomec, Thor Park 8320, B-3600 Genk, Belgium

*Corresponding author. Email: xueshi.jiang@uhasselt.be; bernhard.siegmund@uhasselt.be; koen.vandewal@uhasselt.be

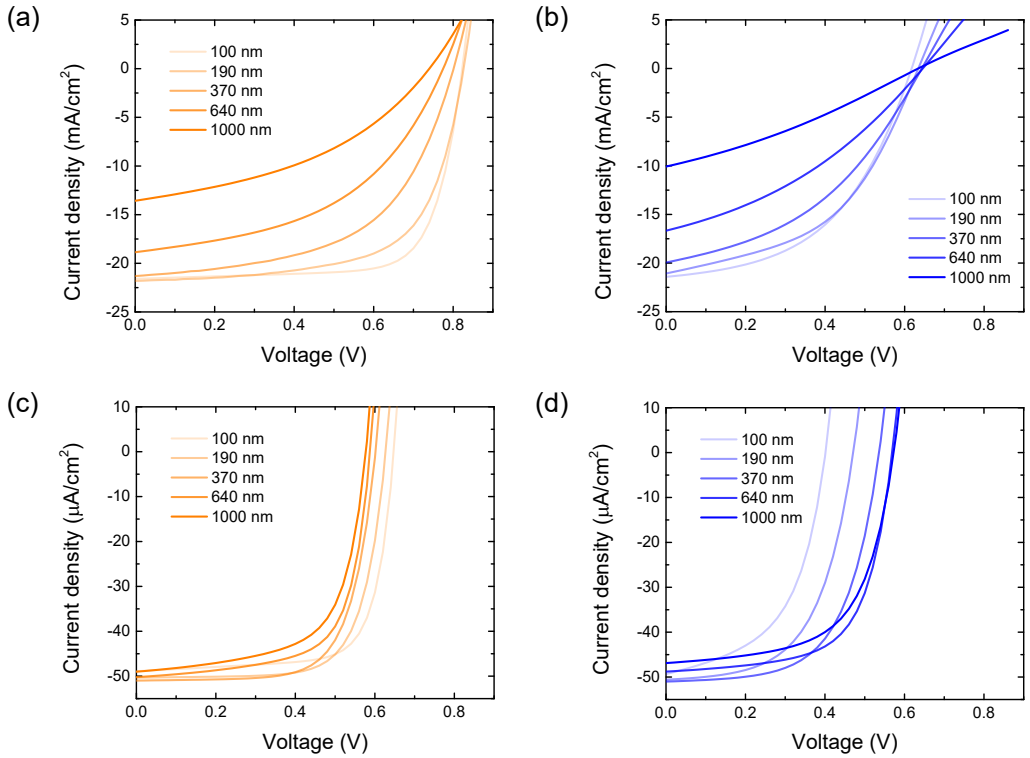

Fig. S1 Current density-voltage characteristics upon absorber thickness variation for devices with ETL under (a) AM 1.5G or (c) 3000 K 450 lux LED and without ETL under (b) AM 1.5G or (d) 3000 K 450 lux LED illumination.

Table S1 Photovoltaic parameters of OPV cells with device architecture ITO/PEDOT:PSS/PM6:IT-4F/(PDINN)/Ag under AM 1.5G illumination. The data represented are averaged over 8 cells.

Light source	P_{in} (mW/cm^2)	Thickness (nm)	ETL	V_{OC} (V)	J_{SC} (mA/cm^2)	FF	P_{out} (mW/cm^2)	PCE (%)	EF
AM 1.5G	100	100	w PDINN	0.823	21.62	0.73	12.94	12.94	2.03
			w/o PDINN	0.616	21.31	0.48	6.36	6.36	
		190	w PDINN	0.817	22.26	0.64	11.69	11.69	1.92
			w/o PDINN	0.634	20.77	0.46	6.09	6.09	
		370	w PDINN	0.793	21.41	0.55	9.39	9.39	1.85
			w/o PDINN	0.637	19.71	0.40	5.08	5.08	
		640	PDINN	0.772	19.63	0.47	7.20	7.20	1.99
			w/o PDINN	0.641	16.09	0.35	3.63	3.63	
		1000	PDINN	0.744	13.36	0.40	4.03	4.03	2.16
			w/o PDINN	0.636	9.77	0.30	1.86	1.86	

Table S2 Photovoltaic parameters of OPV cells with device architecture ITO/PEDOT:PSS/PM6:IT-4F/(PDINN)/Ag under 3000 K 450 lux LED illumination. The data represented are averaged over 8 cells.

Light source	P_{in} (μW/cm^2)	Thickness (nm)	ETL	V_{OC} (V)	J_{SC} (μA/cm^2)	FF	P_{out} (μW/cm^2)	PCE (%)	EF
3000 K 450 lux LED	128.56	100	w PDINN	0.647	49.33	0.73	23.30	18.13	2.27
			w/o PDINN	0.402	48.85	0.52	10.21	8.00	
		190	w PDINN	0.628	50.59	0.71	22.56	17.63	1.68
			w/o PDINN	0.475	49.91	0.57	13.51	10.50	
		370	w PDINN	0.602	50.73	0.69	21.07	16.47	1.33
			w/o PDINN	0.528	50.35	0.60	15.95	12.41	
		640	PDINN	0.587	50.18	0.67	19.74	15.24	1.09
			w/o PDINN	0.570	49.18	0.64	17.94	14.00	
		1000	PDINN	0.576	48.64	0.64	17.93	13.86	1.10
			w/o PDINN	0.571	46.90	0.60	16.07	12.60	

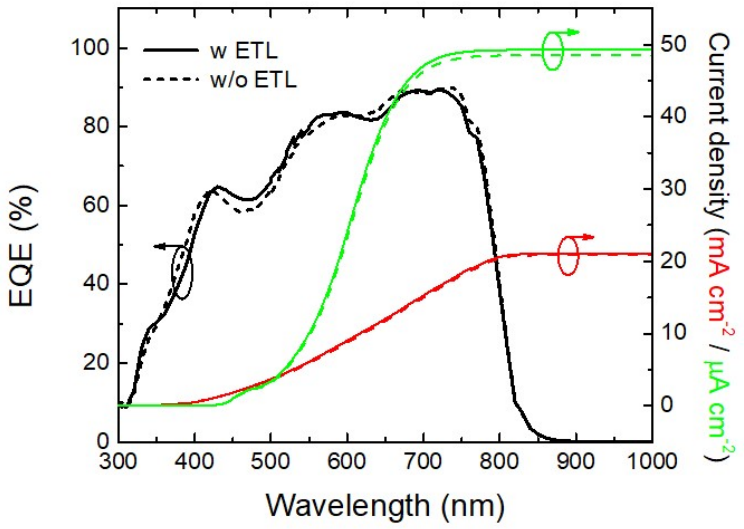

Fig. S2 The external quantum efficiencies (EQE) and integral current densities of devices with 100 nm PM6:IT-4F absorber, with or without the ETL PDINN. The current densities refer to outdoor (red) and indoor (green) illumination, in absence (dashed line) or presence (solid line) of an ETL.

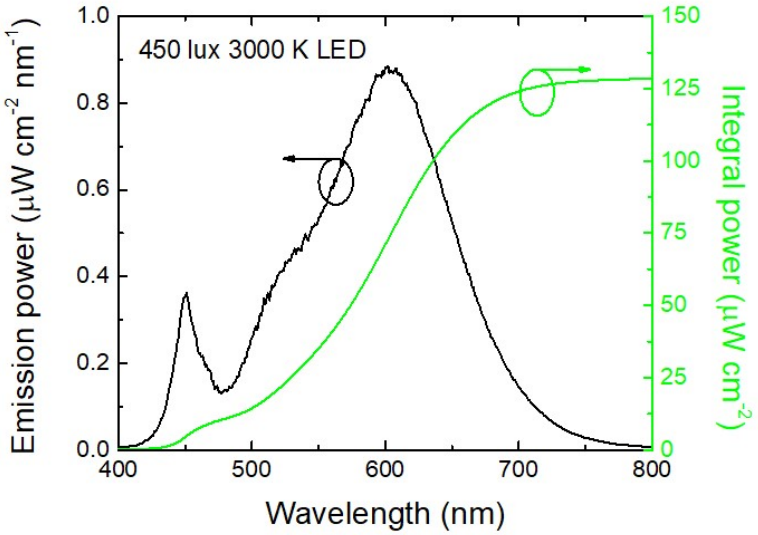

Fig. S3 Emission power spectrum and integrated power spectrum of the 3000 K LED used in this study to simulate indoor illumination at 450 lux.

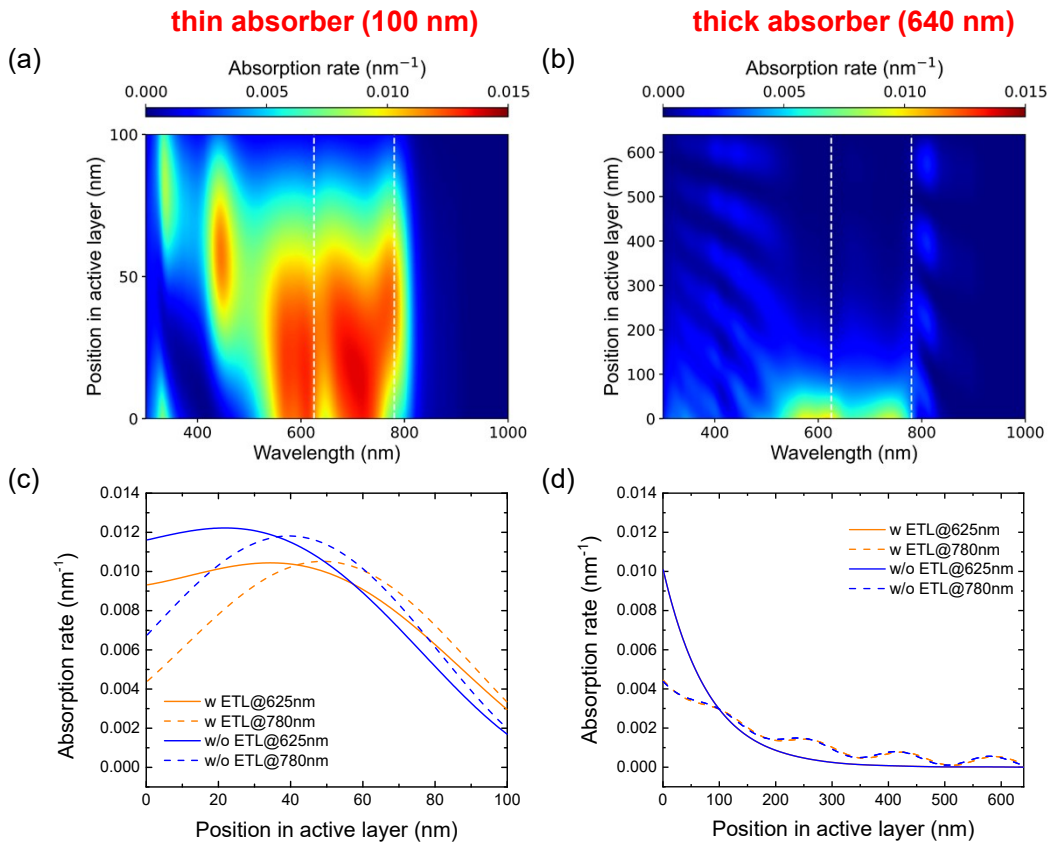

Fig. S4 The simulated spectrally and spatially resolved absorption profile of (a) 100 nm active layer and (b) 640 nm active layer in device architecture: ITO/PEDOT:PSS/PM6:IT-4F/Ag, where the white dashed line indicates the wavelengths used in the monochromatic *J-V* measurements. (c, d) The absorption profiles indicated by the white dashed lines in (a) and (b).

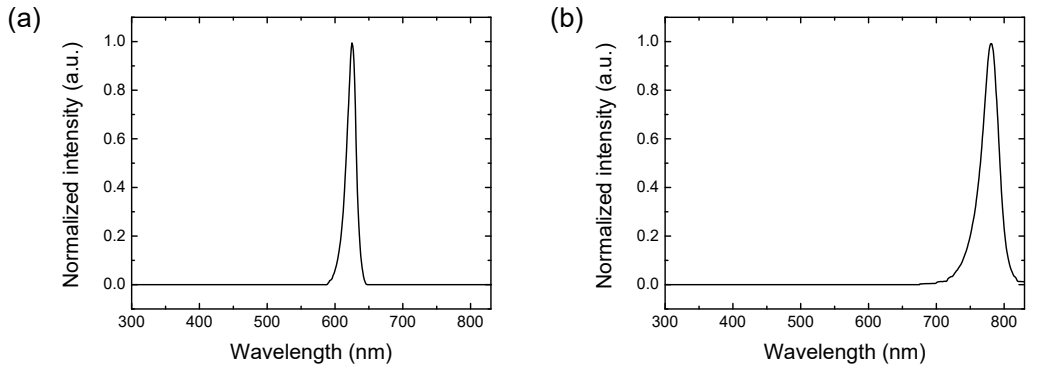

Fig. S5 Spectrum of the (quasi-)monochromatic LED (a) Thorlabs M617L3 and (b) Thorlabs M780L3 used in this study.

Supplementary Note 1. Drift-diffusion simulation

The equations below were solved to simulate the behavior of carriers in the devices, as shown in references.[1, 2]

$$\nabla \cdot \left(\varepsilon_r \varepsilon_0 \nabla \phi\right) = -q\left(p - n + p_t - n_t\right)$$

$$J_n = -D_n \nabla n + \mu_n n \nabla \phi$$

$$J_p = -D_p \nabla p + \mu_p p \nabla \phi$$

$$\nabla \cdot J_n = G - R$$

$$\nabla \cdot J_p = G - R$$

Where ϕ is the electrostatic potential, p and n are hole density and electron density. q, ε_0, ε_r, p_t and n_t are elementary charge, dielectric constant in vacuum, relative dielectric constant, density of trapped holes and trapped electrons, respectively. J_n and J_p are electron and hole particle flux. *G* and *R* are generation rate, which was calculated by using transfer matrix method and recombination rate, respectively.

Both the bimolecular recombination and SRH recombination are included in the model. The SRH recombination is calculated by the equations below.

$$R_{SRH} = \int_{HOMO}^{LUMO} \frac{N_t(E)\left(np - n_i^2\right)}{\frac{1}{C_n}\left(p + p_1\right) + \frac{1}{C_p}\left(n + n_1\right)} dE$$

$$n_1 = N_c \exp\left(\frac{E_t - LUMO}{kT}\right)$$

$$p_1 = N_v \exp\left(\frac{HOMO - E_t}{kT}\right)$$

Where $C_n(C_p)$ denotes the capture coefficients for electrons (holes),[3] $n_1(p_1)$ is the characteristic trap densities contain the trap energetic position E_t, and $N_t(E)$ is the distribution of trap state density.

Besides the bulk traps in the absorber, as the consequence of metal induced gap states (MIGS)

at metal-organic interface,[4, 5] extra traps are introduced in the vicinity of cathode in the simulation of devices without ETL. The width of the region with extra traps is chosen to be 1% of the absorber thickness to ensure that the built-in field is inversely proportional to the absorber thickness.

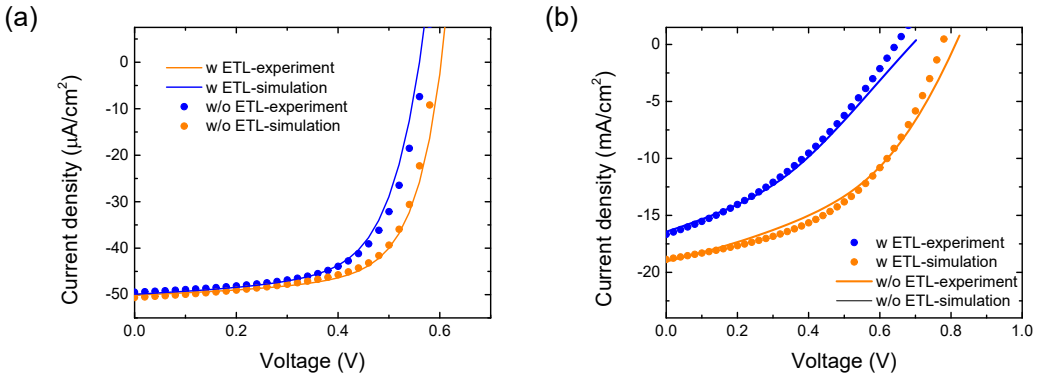

Fig. S6 The simulated and experimental *J-V* characteristics of 640 nm absorber devices with or without ETL under (a) 450 lux LED and (b) AM 1.5G illumination. Series resistance R_s of 5 Ω cm² and shunt resistance R_p of 3.33 MΩ cm² are used in the simulation.

Table S3 Parameters used in the drift-diffusion simulations.

Parameter	Symbol	w ETL	w/o ETL
Bandgap	E_g [eV]	1.18	1.18
Built-in field	V_{bi} [eV]	0.85	0.65
Hole injection barrier	ϕ_h [eV]	0.2	0.2
Electron injection barrier	ϕ_e [eV]	0.13	0.33
Effective density of states of LUMO	N_C [m^{-3}]	9×10^{25}	9×10^{25}
Effective density of states of HOMO	N_V [m^{-3}]	9×10^{25}	9×10^{25}
Surface recombination velocity of minority carriers at anode	S_n [m/s]	0	0
Surface recombination velocity of minority carriers at cathode	S_p [m/s]	0	∞
Hole mobility	μ_h [m^2/Vs]	3×10^{-8}	
Electron mobility	μ_e [m^2/Vs]	8×10^{-8}	
Bimolecular recombination constant	k [m^3/s]	6×10^{-19}	
Generation rate of excitons	G [1/m^3s]	from optical simulation	
Dissociation probability of excitons	P	0.95	
Bulk trap state density	N_t [1/m^3]	8×10^{19}	
The energetic distance between bulk trap level and LUMO	[eV]	0.59	
Bulk electron capture coefficient	C_n [m^3/s]	1×10^{-16}	
Bulk hole capture coefficient	C_p [m^3/s]	1×10^{-16}	
Extra surface trap states density in devices without ETL	$N_{t,extra}$ [1/m^3]	5×10^{24}	
The energetic distance between extra surface trap level and LUMO	[eV]	0.33	
Electron capture coefficient of extra traps	$C_{n,extra}$ [m^3/s]	1×10^{-16}	
Hole capture coefficient of extra traps	$C_{p,extra}$ [m^3/s]	1×10^{-18}	

Supplementary Note 2. Calculation of non-geminate recombination power loss

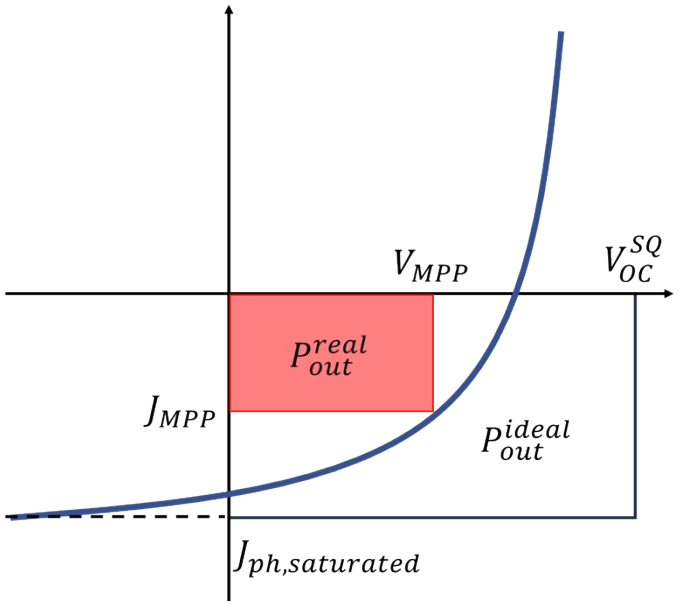

Fig. S7 Schematic *J-V* characteristic to illustrate the calculation of non-geminate recombination power loss.

As depicted in Figure S7, the power losses due to non-geminate recombination are calculated by considering the power difference between real maximum output power and ideal maximum output power (without non-geminate recombination):

$$\begin{aligned} P_{loss} &= J_{ph,saturated} V_{OC}^{SQ} - J_{MPP} V_{MPP} \\ &= (J_{ph,saturated} - J_{MPP}) V_{OC}^{SQ} + J_{MPP} (V_{OC}^{SQ} - V_{MPP}) \\ &= J_{rec} V_{OC}^{SQ} + J_{MPP} V_{rec} \end{aligned}$$

$$J_{rec} = J_{rec,bulk} + J_{rec,surface} \qquad V_{rec} = V_{rec,bulk} + V_{rec,surface}$$

Where J_{MPP} and V_{MPP} denote the current density and voltage at maximum power point, $J_{rec,\,bulk}$ ($J_{rec,\,surface}$) and $V_{rec,bulk}$ ($V_{rec,surface}$) are the current density loss and voltage loss caused by bulk (surface) recombination.

The open-circuit voltage under Shockley-Queisser assumption V_{OC}^{SQ} is the maximum achievable voltage under the illumination of a certain light intensity. V_{OC}^{SQ} is calculated by the equation below[6]:

$$V_{OC}^{SQ} = \frac{kT}{q} \ln\left(\frac{J_{SC}}{J_0^{SQ}} + 1\right) = \frac{kT}{q} \ln\left(\frac{J_{SC}}{q \cdot \int_{E_{gap}}^{\infty} \phi_{BB}(E) dE} + 1\right)$$

The saturated photocurrent $J_{ph,\,saturated}$ is calculated by:

$$J_{ph,saturated} = q \cdot \int G(x) \cdot P dx$$

Where $G(x)$ is the spatial generation profile of excitons and P is the dissociation probability.

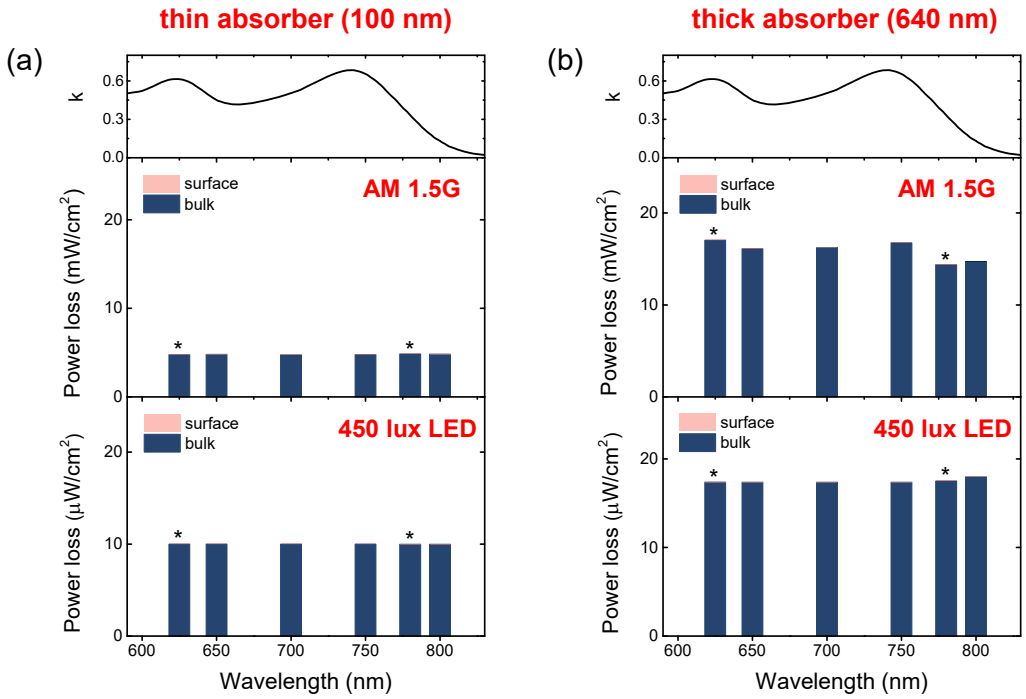

Fig. S8 Simulated non-geminate recombination power loss in a device with ETL under weak and strong monochromatic excitation with (a) 100 nm and (b) 640 nm active layer. The wavelengths used in monochromatic *J*-*V* measurements are indicated by stars.

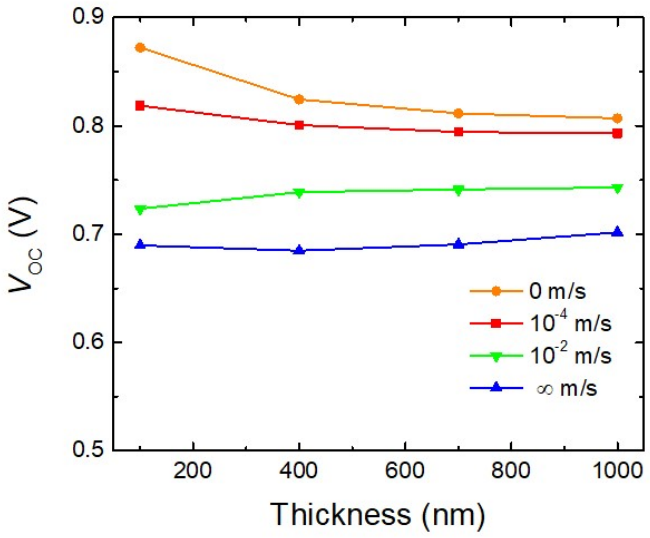

Fig. S9 The open-circuit voltage (V_{OC}) of devices without ETL under AM 1.5G illumination with different surface recombination velocities of minority carriers at the back cathode (S_p), as a function of absorber thickness. If the back cathode is selective (S_p=0 m/s), the V_{OC} decreases as absorber thickness increases due to increased bulk recombination. When increasing S_p, the effect of the reduced surface recombination on V_{OC} arises with increasing absorber thickness, which counteracts the increased bulk recombination. As a consequence, the V_{OC} is nearly independent on absorber thickness for a non-selective back cathode (S_p=∞ m/s).

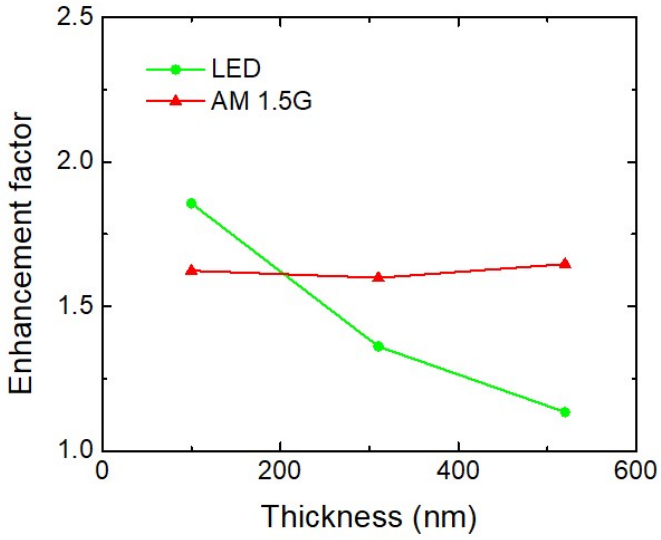

Fig. S10 Evolution of the enhancement factor as a function of active layer thickness under AM 1.5G and LED illumination. The device architecture is ITO/PEDOT:PSS/PM6: Y6/(PDINN)/Ag.

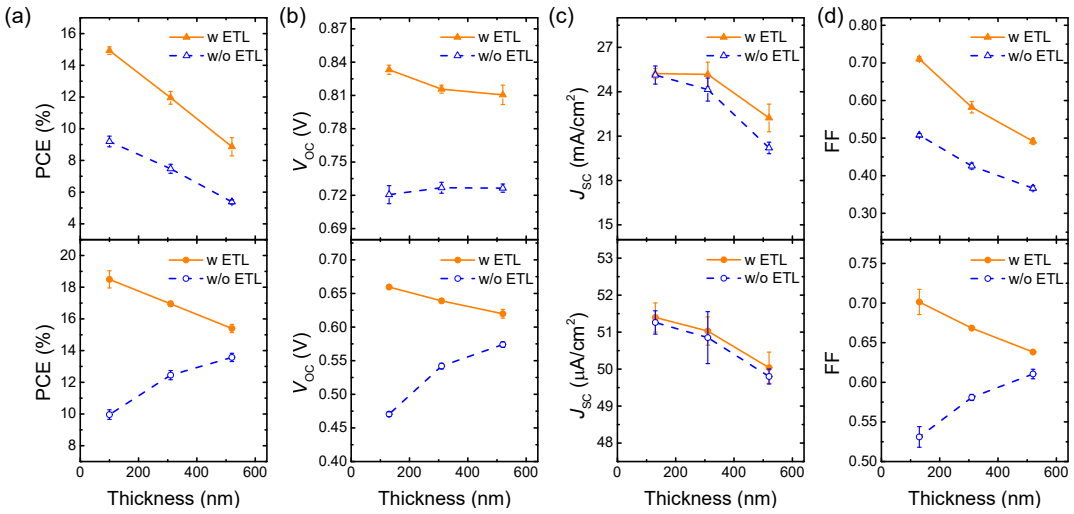

Fig. S11 Photovoltaic performance of devices with or without ETL under AM 1.5G (upper) and 450 lux LED illumination (lower), as a function of active layer thickness: (a) power conversion efficiency, (b) open-circuit voltage, (c) short-circuit current density and (d) fill factor. The devices architecture are ITO/PEDOT:PSS/PM6:Y6/(PDINN)/Ag.

References

1. T. Kirchartz and J. Nelson, in *Multiscale Modelling of Organic and Hybrid Photovoltaics*, eds. D. Beljonne and J. Cornil, Springer Berlin Heidelberg, Berlin, Heidelberg, 2014, DOI: 10.1007/128_2013_473, pp. 279-324.

2. W. Tress, Ph.D. Doctoral thesis, Technical University of Dresden, 2012.

3. M. Kuik, L. J. A. Koster, G. A. H. Wetzelaer and P. W. M. Blom, *Physical Review Letters*, 2011, **107**, 256805.

4. J. Hwang, A. Wan and A. Kahn, *Materials Science and Engineering: R: Reports*, 2009, **64**, 1-31.

5. W. Mönch, *Surf Sci.*, 1994, **299-300**, 928-944.

6. J. Liu, S. Chen, D. Qian, B. Gautam, G. Yang, J. Zhao, J. Bergqvist, F. Zhang, W. Ma, H. Ade, O. Inganäs, K. Gundogdu, F. Gao and H. Yan, *Nature Energy*, 2016, **1**, 16089.